Arabian Journal of Chemistry (2022) **15**, 104297

King Saud University

Arabian Journal of Chemistry

www.ksu.edu.sa
www.sciencedirect.com

ORIGINAL ARTICLE

LC-MS-based multi-omics analysis of brain tissue for the evaluation of the anti-ischemic stroke potential of Tribulus terrestris L. fruit extract in MCAO rats

Dandan Xu [a,b], Yang Wang [c,*], Wenjun Guo [b,d], Xingxing Li [b], Yue Liu [b], Yuqing Han [b], Hongming Zhang [b], Qiyan Wei [b], Yongsheng Wang [a,*], Yajuan Xu [b,*]

[a] *School of Pharmaceutical Sciences, Jilin University, Changchun 130021, China*
[b] *Key Laboratory of Medicinal Materials, Jilin Academy of Chinese Medicine Sciences, Changchun 130021, China*
[c] *Jilin Ginseng Academy, Changchun University of Chinese Medicine, Changchun 130117, China*
[d] *School of Pharmaceutical Sciences, Changchun University of Chinese Medicine, Changchun 130117, China*

Received 24 May 2022; accepted 19 September 2022
Available online 23 September 2022

KEYWORDS

Tribulus terrestris L. fruit extract;
Chemical composition analysis;
Metabolomics;
Proteomics;
Joint pathway analysis

Abstract This study aimed to investigate the chemical composition of Tribulus terrestris L. fruit (TT) extract named TT15 and its protective effect against ischemic stroke (IS) as well as corresponding mechanisms. The chemical composition of TT15 was analyzed by liquid chromatography-mass spectrometry (LC-MS), and the compound identification was conducted via searching the in-house database. The LC-MS-based multi-omics approach was applied to search the differential metabolites and differential proteins in rat brain tissue and to explore the biomarker and molecular mechanism of TT15 against middle cerebral artery occlusion (MCAO). A total of 20 compounds were identified from TT15, mainly including alkaloids, flavonoids, phenols, quinones, and esters. These 20 compounds significantly affected the metabolism of 44 metabolites and the expression of 51 proteins. Joint pathway analysis showed that these metabolites and proteins were mainly involved in the response to elevated platelet cytosolic Ca^{2+} and platelet activation, which inferred that TT15 may exert a protective effect against cerebral ischemic injury via regulating platelet function. This study provides useful information for further exploration of the mechanisms of TT extract against IS.

* Corresponding authors.
E-mail addresses: wangyang@ccucm.edu.cn, white-wing@163.com (Y. Wang), wys@jlu.edu.cn (Y. Wang), xyj6492@126.com (Y. Xu).
Peer review under responsibility of King Saud University.

Production and hosting by Elsevier

https://doi.org/10.1016/j.arabjc.2022.104297
1878-5352

1. Introduction

With a mortality rate of about 25 % and a morbidity rate of about 5 %, stroke is the third major cause of disability and the second leading cause of death (Yang et al., 2021). It is classified into two major categories: ischemic stroke (IS) and hemorrhagic stroke, and About 87 % of cases are thought to be caused by ischemia (Neuhaus et al., 2017). In recent years, increasingly recognized cases of stroke were found in young people (Caplan and Biousse 2004), which makes treatment and prevention of IS increasingly crucial. Stroke can be caused by a variety of factors and mechanisms, including energy metabolism disorders, excitotoxicity, oxidative stress, Ca^{2+} overload, blood–brain barrier (BBB) leakage, mitochondrial damage and dysfunction, and neurovascular unit (NVU) damage. These factors and mechanisms all have connections and interact with one another (Zhu et al., 2020). Currently, IS can be effectively treated with thrombolysis and thrombectomy. However, these techniques can only be used in 15 % of patients, because of the short time windows limitation. Furthermore, many compounds have shown neuroprotective effects in preclinical research but have yet to be translated into effective medicines(Fluri et al., 2015). Therefore, there is an urgent need for therapeutic strategies that are broadly applicable to IS. The ''one medicine, one target'' approach is particularly challenging to apply in the context of these complicated elements and their interactions, leading to unfavorable outcomes in the treatment of stroke (Chen et al., 2017; Chen et al., 2020).

Traditional Chinese medicine (TCM) has been utilized for thousands of years to treat people with stroke-like symptoms and clinical traits in China and East Asia. TCM has a lot of unique benefits in the treatment of IS, including multi-site, multi-component, multi-level, and multi-target comprehensive treatment and overall regulation. Many researchers have studied extracts of TCM and their effective components for the treatment of IS and have achieved remarkable results (Yang et al., 2016; Xie et al., 2021a; Xie et al., 2021b). Tribulus terrestris (TT) is an annual creeping herb that has a variety of uses in China, including depression relief, blood activation and wind dispelling, eyesight brightening, and itching relief. We have conducted a series of studies to investigate the effective components and underlying mechanisms of TT against IS, with a special focus on the gross saponins that contain a mixture of dozens of different types of saponins. Employing metabolomics, proteomics, network pharmacology, and molecular docking approaches, the results demonstrated the therapeutic and protective effect of the gross saponins against IS (Wang et al., 2019; Guo et al., 2020; Wang et al., 2021). During our recent activity screening pilot experiment, we found that other compositions besides saponins also showed good anti-IS activity, such as TT15 isolating from TT. Therefore, in this study, we focused on TT15, including the analysis of its chemical composition, the evaluation of its anti-IS effects as well as the corresponding potential mechanisms.

Advanced integrated omics approaches could offer fresh perspectives on the pathophysiology and physiology of stroke, allowing the characterization of a wide range of molecular regulatory disorders, and they also are able to identify novel factors linked to IS (Ludhiadch et al., 2020). Integrated omics entails looking at the biological relationships in metabolites (metabolome) and proteins (proteome) simultaneously and showing their interaction at the molecular level. The identification of therapeutic targets and the discovery of biomarkers could provide useful information on the therapeutic mechanisms of TT15 against IS.

In the present integrated omics study, an MCAO rat model with IS was constructed to evaluate the protective effect of the TT15 via tail vein injection. Metabolites were detected by ultra-high performance liquid chromatography equipped with quadrupole-Orbitrap mass spectrometry (UHPLC-Q-Orbitrap/MS) to investigate the protective biomarkers and the metabolic pathway of IS. The tandem mass tags (TMT)-based proteomics analysis was applied to observe the proteins and further search for the therapeutic targets and the protection mechanisms of the TT15 against IS. This study provides a new perspective for better understanding the process of IS and the therapeutic mechanisms of TT15 on IS.

2. Material and methods

2.1. Materials

HPLC-grade acetonitrile, methanol, and formic acid were purchased from Fisher Scientific Corporation (Loughborough, UK). Ultrapure water was prepared using a Milli-Q purification system (Billerica, MA, USA).

2.2. Preparation of TT15

The active fraction of TT fruit named TT15 was manufactured by ourselves. Primarily, the TT fruit was ground to a coarse powder and extracted with 70 % aqueous ethanol. The extract solution was filtered and concentrated. The concentrated sample was diluted in 10 % acetonitrile aqueous solution and separated using an octadecylsilyl column, and then successively eluted with different concentrations of aqueous acetonitrile solution. The TT15 was eluted with 15 % aqueous acetonitrile. All fractions were collected and dried under vacuum at 75 °C for further use. For the LC-MS analysis, 1.25 mg of TT15 sample were dissolved in 1 mL 50 % aqueous ethanol, then centrifuged at 10 000 g for 5 min at 4 °C. One microliter supernatant was used for LC-MS analysis.

2.3. Animals and treatments

A total of 30 adult male Wistar rats, weight 250 ± 20 g, were purchased from Changsheng Biotechnology Co. ltd (Liaoning, China). Animals were kept at room temperature (21 ± 2 °C) and humidity (50 ± 10 %) with 12/12 h light/dark cycles and fed standard rat chow and water ad libitum. All treatments of animals were approved by the Animal Ethics Committee, Academy of Traditional Chinese Medicine of Jilin Province (approval No. JLSZKYDWLL-2018–015).

The animal treatment and MCAO model establishment were performed by using our former method (*see* supplemental material). After two weeks of acclimatization, all rats were randomly divided into three groups, including the Sham group, the Model group, and the TT15 group. Administration of TT15 (3 mg/kg) was performed via tail vein injection for three days before and 24 h after the MCAO operation for TT15 rats. The sham-operated and MCAO rats were administrated with the same volume of saline.

The neurological function score and brain cerebral infarction area of rats in the three groups were measured. The remaining brain tissue was collected and stored at −80 °C.

2.4. LC and LC-MS analysis of TT15

The TT15 was analyzed by UHPLC-Q-Orbitrap/MS. An aliquot of 1 μL TT15 solvent was injected into a Vanquish Duo UHPLC system (Thermo Fisher Scientific, San Jose, CA, USA) equipped with a Waters ACQUITY HSS T3 column (1.8 μm, 2.1 × 100 mm) at 25 °C. The mobile phase

consisted of 0.1 % aqueous formic acid (phase A) and acetonitrile (phase B) under the following gradient program: 0–5 min, 6 % B; 5–15 min, 6 %-9% B; 15–25 min, 9 %-10 % B; 25–35 min, 10 %-11 % B; 35–45 min, 11 %-12 % B; 45–55 min, 12 %-13 % B; 55–65 min, 13 %-14 % B; 65–75 min, 14 %-95 % B; 75–90 min, 95 % B. The flow rate was set at 0.3 mL/min, and UV detection was applied at 254 nm.

The mass spectrometer was operated in positive ion modes, and the profile data was recorded at the range of m/z 50–750. The full scan acquisition was performed at the resolution of 35 000, while the tandem MS information was acquired under ddMS2 (TOP 10) mode with a resolution of 17 500, and the ramped normalized collision energy (NCE) of 25–45. MS parameters setup were as follows, Sheath gas flow rate was 40, Aux gas flow rate was 15, Spray voltage was 3.25 kV, Capillary temperature was 250 °C, and the Aux gas heat temperature was set as 350 °C. Before sample analysis, the mass spectrometer was calibrated using the vendor-provided Pierce™ calibration solution (Thermo Fisher Scientific, San Jose CA, USA).

The compound identification was conducted by comparing the MS and MS/MS information with our established in-house database. The chemical composition of TT was collected by searching the database of Pubmed and China National Knowledge Infrastructure (CNKI). Then the obtained information was input into TraceFinder software to establish an in-house database. After UHPLC-MS analysis, the raw data was imported into the TraceFinder database, the m/z of compounds was matched automatically in 5 ppm default error, and their MS and tandem MS information were manually examined. And some of the identifications were further confirmed using standard references.

2.5. LC-MS-based multi-omics analysis of brain tissue

The aqueous and organic extracts of brain tissue were obtained using the different solvent systems. Then the UHPLC-Q-Orbitrap/MS was used to analyze these two types of extracts separately. The raw data obtained from LC-MS was processed using Compound Discoverer software (CD 3.0, Thermo Scientific) to perform peak extraction, alignment, and normalization, and then exported into a dataset containing sample codes, peak labels, and peak intensities. The obtained dataset was imported into SIMCA software (version 13.0, Umetrics, Umeå, Sweden) for multivariate statistical analysis. After biomarkers were screened out, the metabolite annotation was performed by matching MS and MS/MS information via searching databases. The annotated metabolites were then imported into the MetaboAnalyst network tool (Chong et al., 2018) for pathway analysis.

The protein extracted from brain tissue was analyzed by a NanoLC-MS instrument. The raw data were searched using Proteome Discoverer (PD) software version 2.1 (Thermo Scientific) with the Mascot version 2.6 search engine (Matrix Science, Boston, Massachusetts, USA) against the UniProt Rattus Norvegicus database_20180123. After the differentially expressed proteins (DEPs) were screened out, the Gene Ontology (GO) annotation and KEGG pathway enrichment analysis were performed on the DEPs by using the Metascape web tool (Zhou et al., 2019).

The detailed parameters of the above analyses were listed in the supplemental material.

3. Results

3.1. LC-MS analysis of TT15

As shown in Fig. 1A, several peaks were separated by LC analysis. Then the LC-MS detection was performed using the same separation method to identify the main compounds, and the corresponding BPC was shown in Fig. 1B. After in-house database searching, 20 labeled peaks were identified and 5 of them were confirmed with reference substances. As listed in Table S1, 20 compounds belong to 5 classifications, including eight alkaloids, seven flavonoids, three phenols, one quinone, and one ester.

3.2. The effect of TT15 on MCAO in rats

The effects of TT15 on MCAO rats were evaluated by neurological function score and cerebral infarct size. As shown in Fig. 2A, the rats in the Sham group do not have any neurological defects. The Model group scored the highest out of the three groups, showing that there was a neurological deficit following the MCAO operation. After TT15 administration, the neurological function score significantly decreased from 2.16 ± 1.17 to 1.31 ± 0.60, indicating that TT15 has a neuroprotective effect.

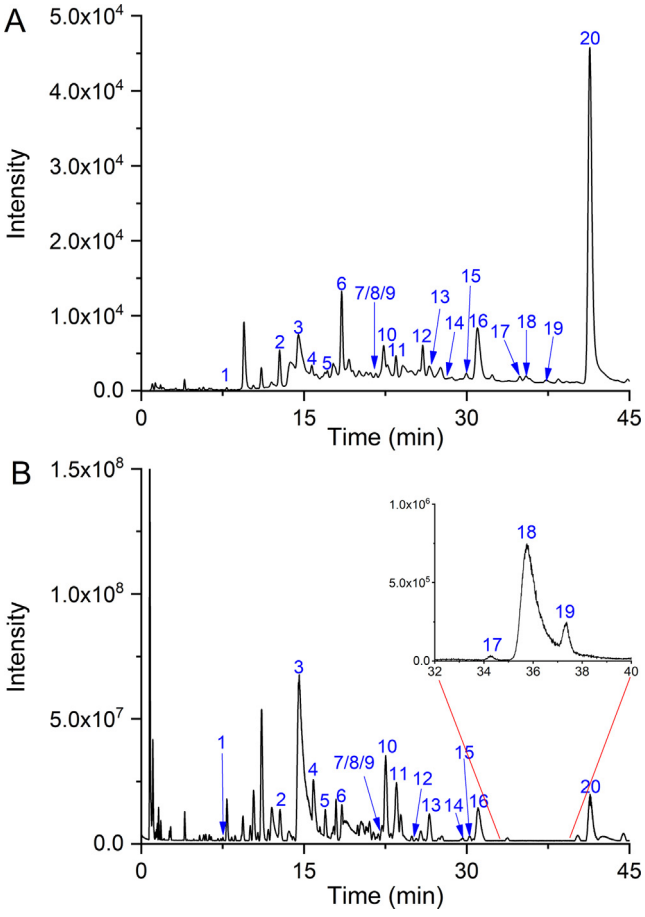

Fig. 1 The LC chromatogram (A) and LC-MS base peak ion chromatogram (B) of TT15.

The typical results of infarct size from each group were presented in Fig. 2B. The infarction locations in the coronal portion are represented by the white patches. Fig. 2C shows the percentage of infarction area in rats. All of the rats in the Model group displayed severe cerebral infarction, with an infarct ratio of 31.74 ± 17.55 %. Rats treated with TT15 showed a considerable reduction in the infarct ratio (19.19 ± 16.19 %). These results indicated that the TT15 has a protective effect against MCAO.

3.3. Metabolomics analysis

3.3.1. Metabolome profile of brain tissue

The reproducibility and stability of the LC-MS method are important prerequisites for metabolomics studies. In this study, the quality control (QC) sample was used for method evaluation. Five QC samples were initially run for system equilibrium, followed by one QC sample run after every-four sample data collections to provide a dataset for method validation. As shown in Fig. S1, relatively tight aggregation of QC samples among all samples was observed, indicating that the developed method has good repeatability and stability in both positive and negative ion modes.

The brain tissue metabolites were analyzed by the validated LC-MS method, and the BPC in both positive and negative ion modes were shown in Fig. S2, a good separation in 25 min was achieved under the established data acquisition method. A few differences were observed among groups, but the visual inspection was not enough to evaluate the effect of TT15. Thus we applied multivariate statistical analysis to assess the variation of the brain tissue metabolites in different groups.

As shown in Fig. 3, there is an obvious separation between the Sham group and the Model group, indicating the metabolic disorder occurred during the modeling process. The samples displayed a propensity to diverge from the MCAO rats and were close to the Sham group following treatment with TT15 (Fig. 4). And TT15 showed a stronger ability to regulate organic extract since the organic extracted samples were closer to the Sham group compared with the aqueous extracted samples. These findings indicated that the TT15 could recover the metabolic changes to normal states mainly through regulating the metabolism of organic metabolites.

3.3.2. Biomarker selection and metabolic pathway analysis

From the comparison of the Model group and the Sham group, the features that fulfilled variation importance in the project (VIP) > 1.5, fold change value (FC) > 1.5, and $P < 0.05$ were screened as potential disease markers. The features that met the same criteria from the comparison of the TT15 group and Model groups were considered as the markers of potential drug efficacy. The intersection of two sets of makers was selected as potential biomarkers, which were used to evaluate the protective effect of TT15 against MCAO in rats. Then these features were annotated by database searching using accurate m/z, MS/MS information, isotope distribution, etc. A total of 44 metabolites were annotated, and their detailed information and change trends in different groups were listed in Table 1. After being treated with TT15, 36 metabolites that were significantly altered due to cerebral ischemia were dramatically reversed.

For visualizing the variation tendency of the biomarker among the three groups, a heat map was constructed based on the relative intensity of metabolites. As shown in Fig. 5A, the color differences indicate the metabolic disturbance in the three groups. The similar colors in Sham and TT15 groups suggested that TT15 can improve the metabolites disorders back to normal.

The result of pathway analysis is shown in Fig. 5B, the metabolic pathways disturbed by MCAO surgery mainly include alanine, aspartic acid and glutamic acid metabolism, glycerol phospholipid metabolism, tryptophan metabolism, and so on.

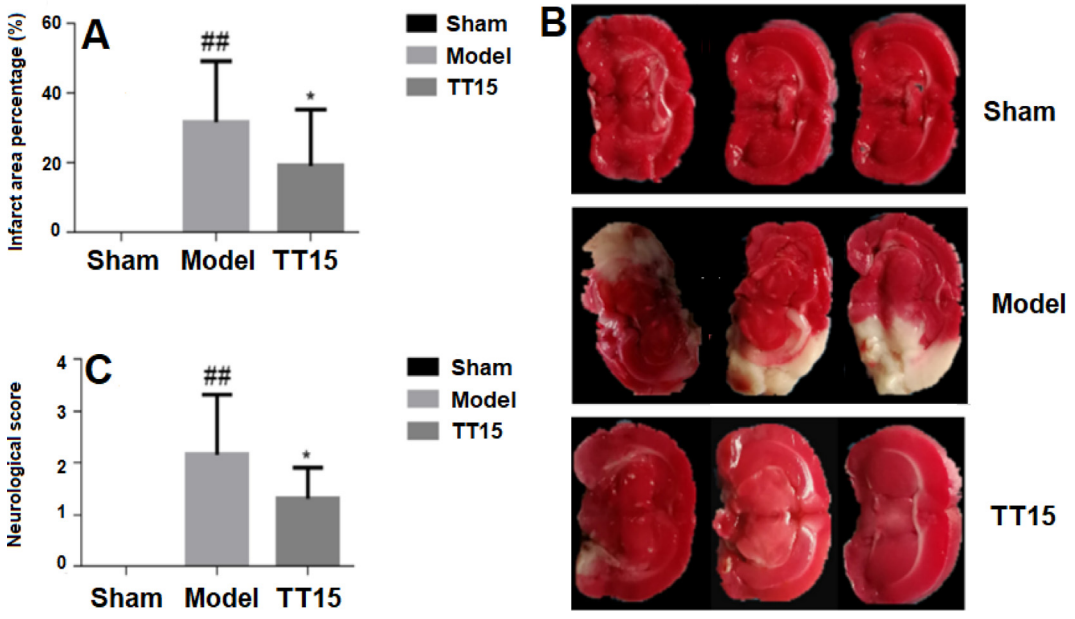

Fig. 2 The effect of TT15 on MCAO, cerebral infarct size (A), representative TTC staining of brain tissue (B), and neurological function score (C). $^{\#\#}P < 0.01$, Model vs Sham group; $^{*}P < 0.05$, TT15 vs Model group.

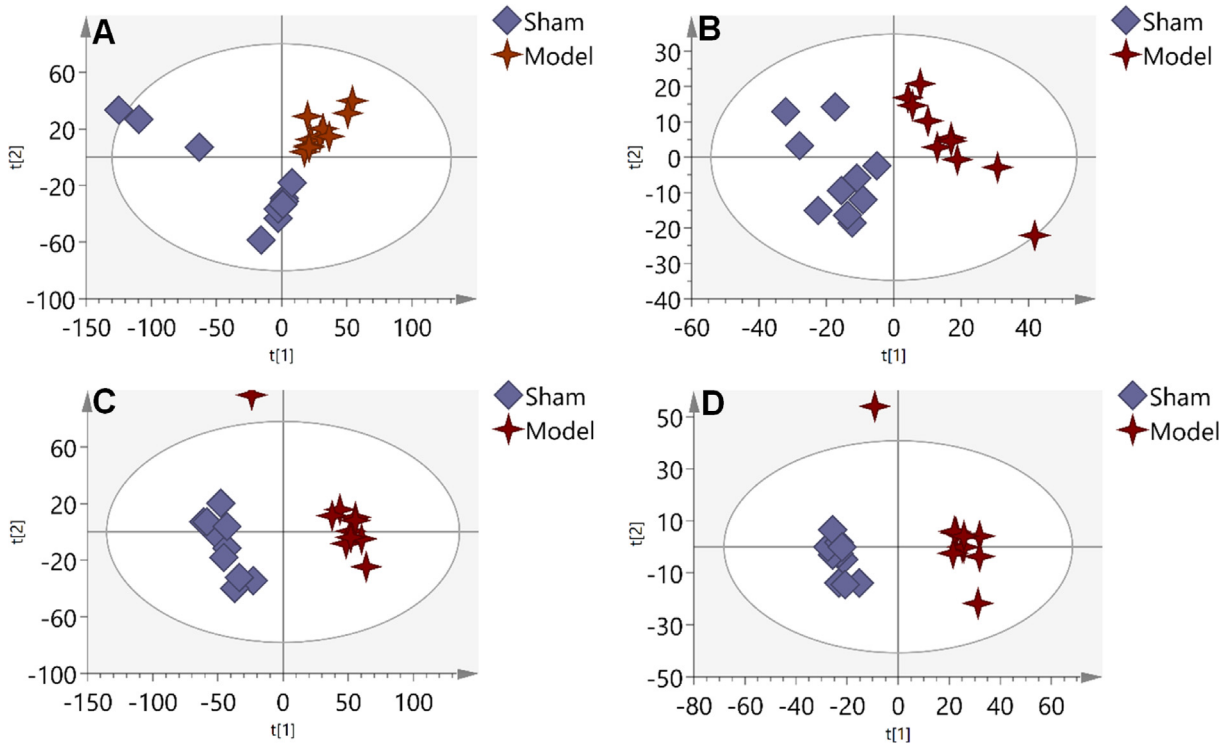

Fig. 3 PLS-DA score plots of Sham group and Model group based on the data acquired from aqueous extracts (A, ESI + , and B, ESI-), and organic extracts (C, ESI + , and D, ESI-).

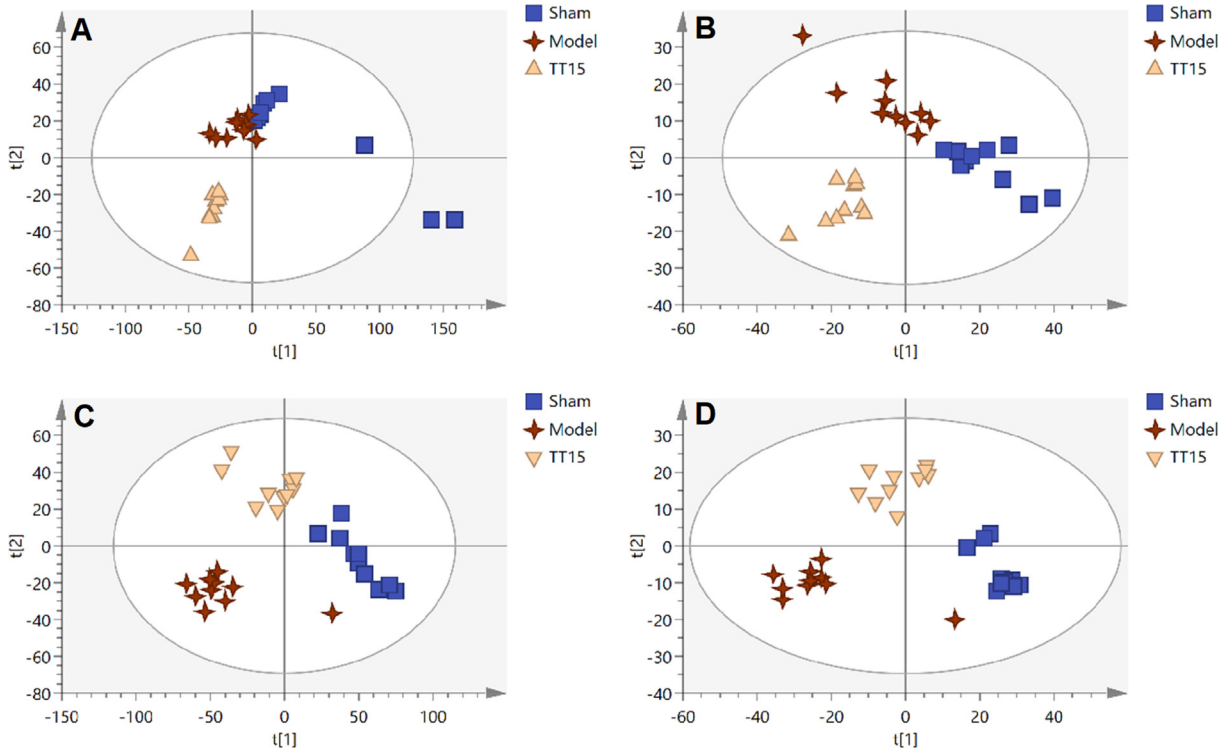

Fig. 4 PLS-DA score plots of Sham group, Model group, and TT15 group based on the data acquired from aqueous extracts (A, ESI + , and B, ESI-) and organic extracts (C, ESI + , and D, ESI-).

Table 1 Annotated endogenous metabolites and their change trends in different groups.

No.	Metabolite	Formula	Exact mass	HMDB ID	Model/ Sham	TT15/ Model	Type
1	Argininic acid	C6H13N3O3	175.09553	HMDB0003148	↑***	$\uparrow^{\#\#}$	Aqueous extract
2	N,N-Dimethylarginine	C8H18N4O2	202.14290	HMDB0001539	↑***	$\uparrow^{\#\#}$	Aqueous extract
3	Cysteineglutathione disulfide	C13H22N4O8S2	426.08793	HMDB0000656	↓**	$\downarrow^{\#}$	Aqueous extract
4	Glutamylglutamic acid	C10H16N2O7	276.09559	HMDB0028818	↓***	$\downarrow^{\#\#}$	Aqueous extract
5	Acetyl arginine	C8H16N4O3	216.12211	HMDB0004620	↓**	$\uparrow^{\#}$	Aqueous extract
6	18-HETE	C20H32O3	320.23272	HMDB0006245	↑**	$\downarrow^{\#\#\#}$	Aqueous extract
7	g-Glutamyltyrosine	C14H18N2O6	310.11887	HMDB0011741	↑***	$\downarrow^{\#\#}$	Aqueous extract
8	Pregnanetriol	C21H36O3	336.26622	HMDB0006070	↑**	$\downarrow^{\#}$	Aqueous extract
9	PS(40:6)	C46H78NO10P	835.53628	HMDB0010167	↑**	$\downarrow^{\#\#}$	Aqueous extract
10	LysoPI(20:4/0:0)	C52H98NO8P	620.29616	HMDB0008356	↑**	$\uparrow^{\#\#}$	Aqueous extract
11	1-Stearoylglycerophosphoserine	C24H48NO9P	525.30733	HMDB0061698	↑***	$\downarrow^{\#\#\#}$	Aqueous extract
12	PS(44:12)	C50H74NO10P	879.50501	HMDB0012450	↑***	$\downarrow^{\#\#}$	Aqueous extract
13	PS(38:4)	C44H78NO10P	811.53737	HMDB0010165	↑***	$\downarrow^{\#}$	Aqueous extract
14	PA(35:2)	C45H86NO7P	686.48898	HMDB0011455	↑***	$\downarrow^{\#\#\#}$	Aqueous extract
15	Sulfanilic acid	C43H80NO7P	173.01491	HMDB0011448	↓***	$\uparrow^{\#}$	Aqueous extract
16	Castanospermine	C8H15NO4	189.10009	HMDB0249700	↑**	$\uparrow^{\#\#\#}$	Aqueous extract
17	Acetyl-DL-carnitine	C9H18NO4	203.11566	HMDB0000201	↑**	$\uparrow^{\#\#\#}$	Aqueous extract
18	N4-Acetylcytidine	C11H15N3O6	284.08621	HMDB0005923	↑*	$\downarrow^{\#}$	Aqueous extract
19	5,6-dihydroxy-2-indolecarboxylic acid	C9H7NO4	193.03763	HMDB0001253	↑***	$\uparrow^{\#\#\#}$	Aqueous extract
20	Proline	C5H9NO2	115.06366	HMDB0000162	↓***	$\uparrow^{\#\#}$	Organic extract
21	Aspartic acid	C4H7NO4	133.03872	HMDB0000191	↓***	$\uparrow^{\#\#\#}$	Organic extract
22	Glutamic acid	C8H13N3O3	147.05457	HMDB0060477	↓***	$\uparrow^{\#\#}$	Organic extract
23	2-Aminomuconic acid	C6H7NO4	157.03893	HMDB0001241	↓***	$\uparrow^{\#\#\#}$	Organic extract
24	Methionine sulfoxide	C5H11NO3S	164.98239	HMDB0002005	↓***	$\uparrow^{\#\#\#}$	Organic extract
25	Guanidino succinic acid	C5H7N3O4	174.05231	HMDB0302618	↓***	$\uparrow^{\#\#\#}$	Organic extract
26	Indoleacrylic acid	C11H9NO2	187.06531	HMDB0000734	↓***	$\uparrow^{\#\#\#}$	Organic extract
27	Tryptophan	C11H12N2O2	204.09186	HMDB0000929	↓***	$\uparrow^{\#\#}$	Organic extract
28	Methoxsalen	C12H8O4	216.04194	HMDB0014693	↓***	$\uparrow^{\#\#\#}$	Organic extract
29	Homocarnosine	C10H16N4O3	240.12443	HMDB0000745	↓***	$\uparrow^{\#\#}$	Organic extract
30	Inosine	C10H12N4O5	268.08311	HMDB0000195	↓***	$\uparrow^{\#\#}$	Organic extract
31	LysoPE(18:1/0:0)	C23H46NO7P	479.30565	HMDB0011505	↑***	$\downarrow^{\#\#}$	Organic extract
32	Diglyceride	C31H60O5	664.50994	HMDB0007008	↓***	$\uparrow^{\#\#}$	Organic extract
33	GPE(18:2/20:2)	C43H80NO7P	753.57405	HMDB0011448	↑***	$\downarrow^{\#\#}$	Organic extract
34	Gpcho(36:2)	C40H80NO8P	771.61941	HMDB0000564	↑***	$\downarrow^{\#\#\#}$	Organic extract
35	GPE(18:2/22:1)	C45H86NO7P	783.62086	HMDB0011455	↑***	$\downarrow^{\#\#}$	Organic extract
36	Coenzyme Q9	C54H82O4	794.62791	HMDB0006707	↑***	$\downarrow^{\#\#}$	Organic extract
37	GPE(18:2/24:1)	C47H90NO7P	811.65230	HMDB0011462	↑***	$\downarrow^{\#\#}$	Organic extract
38	PC(42:10)	C50H80NO8P	853.56888	HMDB0008452	↑***	$\downarrow^{\#\#}$	Organic extract
39	Coenzyme Q10	C59H90O4	862.69089	HMDB0001072	↑***	$\downarrow^{\#\#}$	Organic extract

Table 1 (*continued*)

No.	Metabolite	Formula	Exact mass	HMDB ID	Model/ Sham	TT15/ Model	Type
40	PE-NMe(24:0/20:0)	C50H100NO8P	873.71709	HMDB0113713	↑***	$\downarrow^{\#\#\#}$	Organic extract
41	Gpcho(44:3)	C44H84NO8P	881.72460	HMDB0000593	↑***	$\downarrow^{\#\#}$	Organic extract
42	PG(20:3(6,8,11)-OH(5)/i-24:0)	C50H93O11P	900.64727	HMDB0272290	↑***	$\downarrow^{\#\#\#}$	Organic extract
43	TG(62:13)	C65H100O6	976.75760	HMDB0055057	↑***	$\downarrow^{\#\#}$	Organic extract
44	DMPE(38:7)	C33H62O6	789.54243	HMDB0000548	↑***	$\downarrow^{\#\#}$	Organic extract

* $P < 0.05$, ** $P < 0.01$, *** $P < 0.001$, the Model group versus the Sham group;
# $P < 0.05$, $^{\#\#}$ $P < 0.01$, $^{\#\#\#}$ $P < 0.001$, the TT15 group versus the Model group.
The exact mass was inferred from CD software based on the different adduct ions of the metabolite detected by LC-MS.

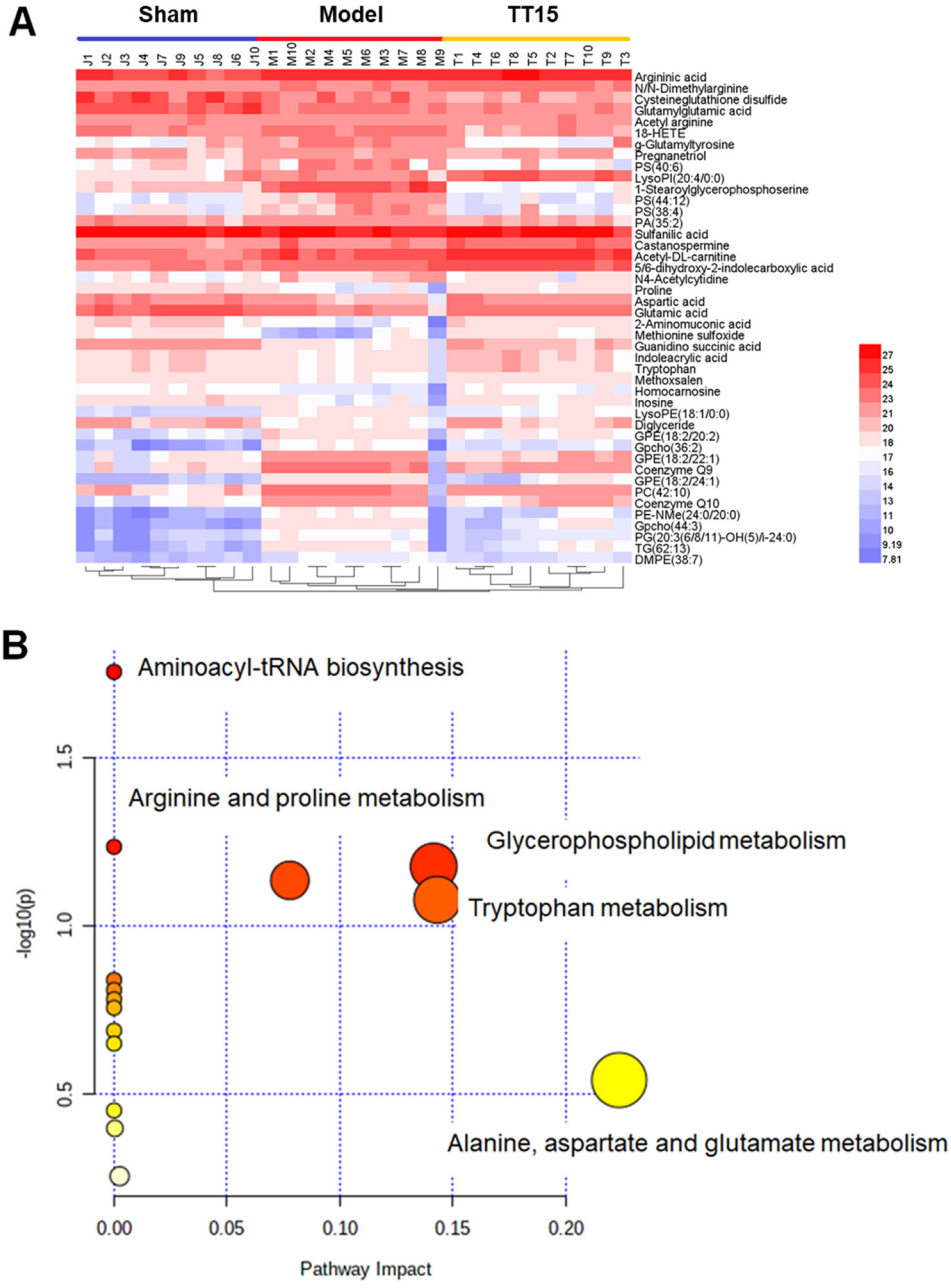

Fig. 5 Heatmap indicated the changes in intensities of the biomarker (A) and the pathway analysis visualized by bubbles plot (B).

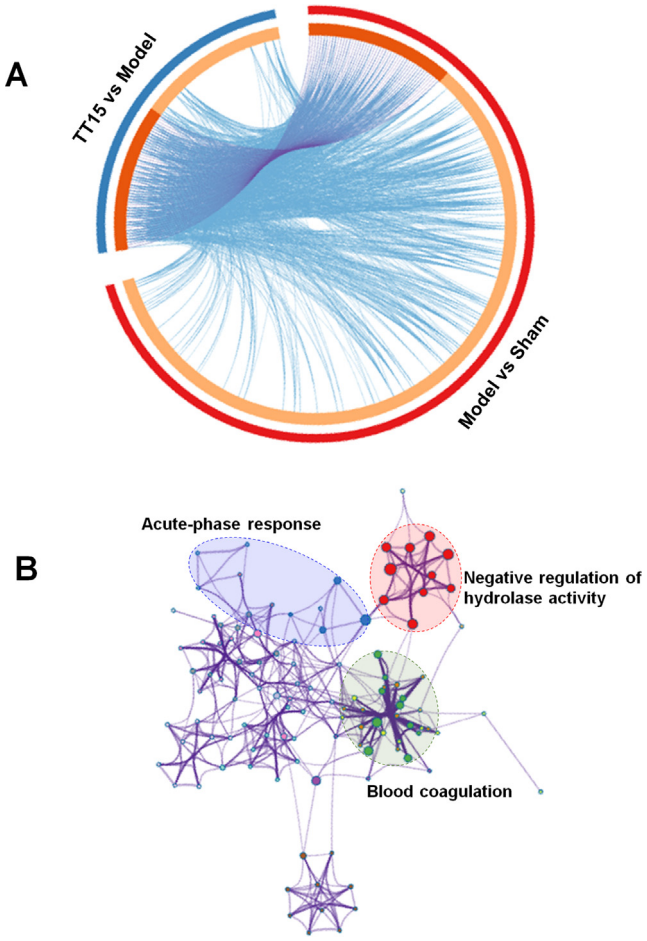

Fig. 6 Circos plot (A) and enrichment network (B) of DEPs.

3.4. Protein expression and bioinformatics analysis

Protein extracts from rat brain tissues were analyzed by TMT-based quantitative proteomics technology. The proteins with FC > 1.2 or FC < 0.83 between the two groups were selected as differentially expressed proteins (DEPs). In the comparison of the Sham group and the Model group, 297 DEPs were filtered out, and 104 DEPs were screened out when the TT15 group was compared to the Model group. Fifty-one overlayed proteins between two sets of DEPs were selected as potential marker proteins and listed in Table S2. The expression of 40 DEPs expressions increased in the Model group, and 35 of them decreased after the TT15 treatment. Meanwhile, the expressions of 11 downregulated proteins were reversed after the treatment with TT15. A Circos graph (Fig. 6A) was constructed to visualize the DEPs distribution between the two comparisons, where each DEP was assigned to a point on the corresponding group of comparison arcs. The purple curve connected the common DEPs in the two comparisons, and the blue curve connected the proteins with different characteristics but sharing the same enrichment process or pathway. The corresponding enrichment network in Fig. 6B shows that the DEPs are greatly associated with negative regulation of hydrolase activity, acute-phase response, blood coagulation, etc.

Functional modules of the DEPs were explored by MCODE, and two clusters, containing 8 and 4 proteins, respectively, were generated (Fig. S3). Proteins in the same cluster are thought to be more intimately connected and interact to execute specific biological functions. For example, proteins in Cluster I were mainly involved in the complement and coagulation cascades pathway; and four proteins in Clusters II belong to keratin. These proteins may have important regulatory roles in the treatment of IS by TT15. Collectively, these results confirmed the protective effect of TT15 on MCAO in rats from the proteomic perspective.

3.5. Joint pathway analysis

To have a better understanding of obvious alteration in the relationships of metabolites and DEPs, we imported potential treatment targets and metabolic biomarkers into the online analysis platform named IMPaLA to accomplish the Joint Pathway Analysis (Kamburov et al., 2011), and further explore pathways involving both the treatment targets and the potential metabolic biomarkers. As shown in Fig. 7, the effect of TT15 is mainly associated with response to elevated platelet cytosolic Ca^{2+}, platelet activation signaling and aggregation, folate metabolism, complement and coagulation cascades, scavenging of heme from plasma and fibrinolysis pathway.

4. Discussion

The MCAO model was successfully established and evaluated by the cerebral infarct size and the neurological function score. TT15 can decrease cerebral infarct size and improve the behavior of MCAO rats. The metabolites and proteins of brain tissues in different groups were analyzed by the LC-MS-based multi-omics method. A total of 44 metabolites and 51 proteins were screened out, and their relative pathways were further studied to explore the protective mechanism of TT15 against MCAO.

4.1. Metabolite profile analysis

In metabolomics, to ensure analysis of as many metabolites as possible, we investigated the metabolic changes of aqueous and organic extract of brain tissue, respectively. The classification of the Sham group and Model group was observed in the PLS-DA score plot, suggesting metabolic disturbance occurred during the MCAO operation. Furthermore, the samples in the TT15 group showed tendencies of separation from the Model group and close to the Sham group, which is consistent with the results in infarct size and neurological score, proving that the TT15 has a protective effect to MCAO. A total of 44 metabolites were screened out as biomarkers via statistical analysis.

The brain is the second most lipid-rich organ in the human body, accounting for about 50 % of its dry weight. Thus, a large number of lipids were screened out as potential biomarkers, including phosphatidylethanolamine (PE), phosphatidylserine (PS), phosphatidylcholines (PC), etc. They are important components of brain tissue that are essential to sustain normal brain function and homeostasis when stroke damage is present. Various lipids, including simple lipids, phospholipids, glycolipids, and fatty acids, are structural components of biological membranes, messengers in cellular signaling pathways, and energy producers. Numerous neurological disorders and neurodegenerative diseases that are characterized by dysregulated lipid

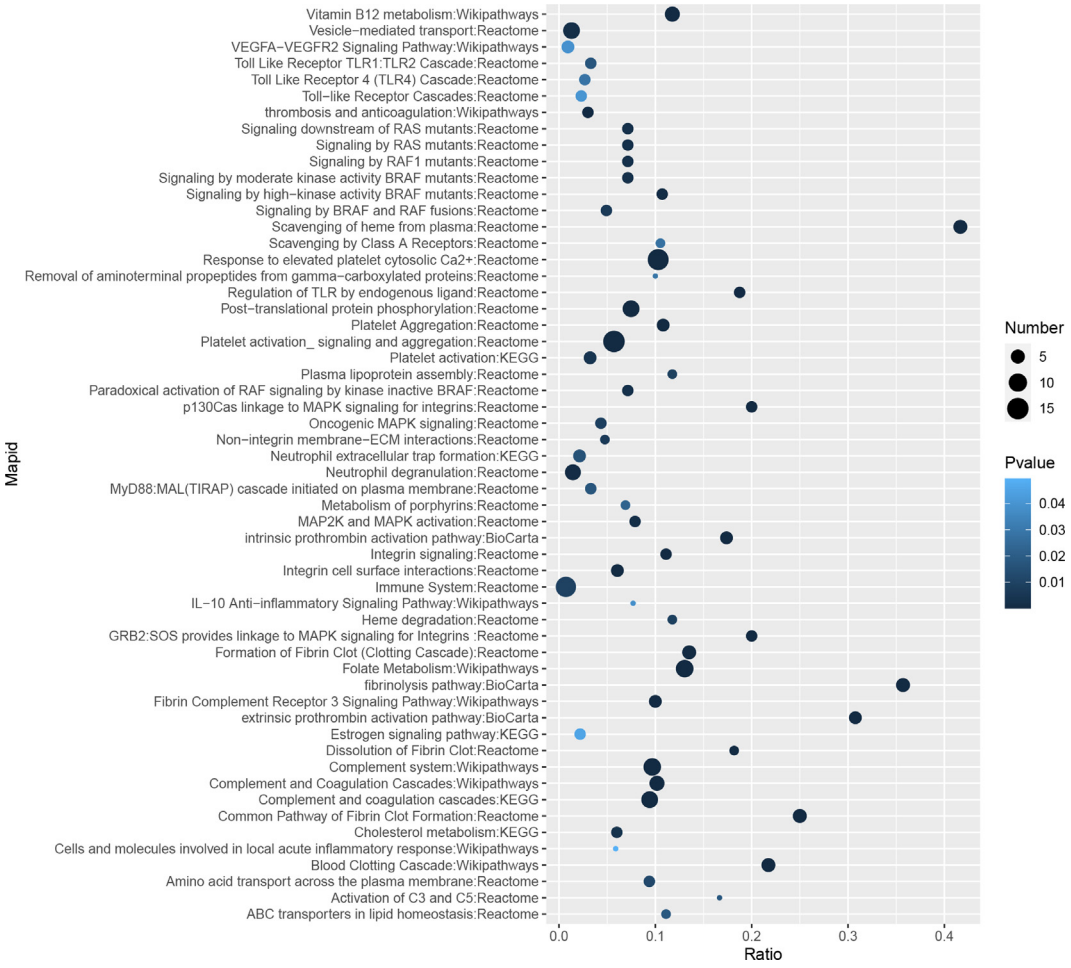

Fig. 7 Bubble maps of the joint pathway analysis.

metabolism have served to highlight the critical role that lipids play in tissue physiology and cell signaling. Alterations in lipid metabolism have been identified as key events leading to central nervous system (CNS) damage such as stroke (Muralikrishna Adibhatla and Hatcher, 2006; Adibhatla and Hatcher, 2007). Numerous metabolomics and lipidomics studies also confirmed the strong relations between lipid metabolism and IS (Au, 2018; Shin et al., 2020).

Several amino acids (AAs) and their derivatives were highlighted. Among them, arginine and its derivatives, glutathione derivatives were reported to be related to oxidative stress in the process of brain tissue injury (Wiesinger, 2001; Reynaert et al., 2006; Van Guldener et al., 2007). The neuroprotective effect of L-arginine administration has been demonstrated through its improvement of cerebral blood flow and reduction of neurological damage after experimental traumatic brain injury (Cherian et al., 2003; Cherian and Robertson, 2003). Glutamic acid, proline, aspartic acid, and tryptophan are associated with neurogenic diseases, and glutamic acid, proline, and aspartic acid belong to excitatory amino acids (EAA) (Victor Nadler et al., 1988; Thomas, 1995; Mattson, 2008). It was reported that the excessive release of EAA was the pathological mechanism behind ischemic brain damage. Reducing the expression of EAA transporter 3 in the rat MCAO model could improve IS (Barahimi et al., 2021). Accelerated degradation of tryptophan and complementary increases in kynurenine metabolites are also frequently observed in serum, cerebrospinal fluid, and/or brain tissue in various diseases such as stroke (Chen and Guillemin, 2009). A clinical study also showed that the tryptophan level was significantly lower in stroke patients than that in the control group (Ormstad et al., 2013). From the perspective of metabolomics, TT15 played an anti-IS role by comprehensively regulating the metabolism of lipids and amino acids, including glycerophospholipid metabolism, arginine and proline metabolism, tryptophan metabolism, etc.

4.2. Protein expression analysis

A total of 51 overlapping DEPs were selected in the comparison of Model vs Sham and TT15 vs Model. As shown in Table S2, the alternation in the expression of proteins proved that TT15 has a protective effect on IS. The PPI network was constructed and two function modules were generated by the MCODE algorithm. As shown in Fig. S3, cluster I contains C3, C4a, Fga, Fgb, and Fgg, etc; and cluster II consists of several keratins.

Apolipoprotein C1 (ApoC1) is an apolipoprotein that plays an active role in the processing of lipids in both endogenous and exogenous environments. It completes this by acting as ligands for cell membrane receptors and regulating the activity of pertinent enzymes, transporters, and lipid transfer proteins. ApoC1 was thought to be closely related to Alzheimer's dis-

ease (AD) and may be a risk factor for the disease. According to a study, both healthy and AD participants' astrocytes and endothelial cells from diverse parts of the human hippocampus expressed ApoC1. In senile plaques from the brains of AD patients, ApoC1 colocalized with β-amyloid and increased the neuronal death brought on by soluble oligomers of β-amyloid. Besides, the ApoC1-deficient mice showed cognitive impairment (Abildayeva et al., 2008; Berbee et al., 2011). Increased levels of ApoC1 are detrimental to arterial arteries, as evidenced by the finding that people at cardiovascular risk also had elevated levels of ApoC1 and myocardial infarction (Fuior and Gafencu, 2019). Similar results were observed in the present study, ApoC1 was up-regulated in the Model group and was down-regulated after being treated with TT15.

C3 is a component in the complement system that can be triggered by various stimuli via three distinct recognition pathways, including the classical, the alternative, and the lectin pathways. (Ricklin et al., 2010). Studies on numerous disorders, including stroke, traumatic brain injury, multiple sclerosis, and AD, revealed a connection between complement system activation and the inflammatory response. (Alawieh et al., 2018; Dalakas et al., 2020). And numerous studies regarded C3 as their main target for the treatment of IS (Gomez-Arboledas et al., 2021). In addition to its several advantageous roles in maintaining brain homeostasis, the complement system was also linked to neurodegeneration. In the CNS, complement proteins are generated by neurons, microglia, astrocytes, and oligodendrocytes (Veerhuis et al., 2011; Berkowitz et al., 2021), and multiple complement proteins (such as C3 or C4) were discovered to be raised in the brains of patients with Huntington's Disease (HD), AD and PD (Ma et al., 2019; Gomez-Arboledas et al., 2021). In the present study, the up-regulated C3 and C4 expression in the Model group were reduced after being treated with TT15, which suggested that the level of C3 and C4 could be potential predictors of outcome after IS.

Fibrinogen (Fg) is made up of two sets of three different polypeptide chains, Fga, Fgb, and Fgg (Kopyta et al., 2014), which plays a significant role in blood clotting and circulation through interaction with platelets. Besides, through its influence on a variety of cellular receptors, including integrins, intracellular adhesion molecule-1, and vascular endothelial cadherin, Fg has been recognized as a key regulator of inflammation, wound healing, angiogenesis, and neoplasia (Krishnamoorthy et al., 2011). Fg can promote atherosclerosis and thrombosis, and the plasma levels of Fg are well-known risk factors for arterial thrombosis (Koster et al., 1994). According to the worldwide genome-wide association studies (GWAS) Catalog, variations of *FGG* were linked to thromboembolism, glycine, and fibrinogen levels; and variants of *FGA* were linked to stroke, thromboembolism, and fibrinogen levels (Abu-Farha et al., 2020). Recently, the roles of *FGB* polymorphisms in IS were intensively analyzed. It was reported that −148C/T and −455G/A polymorphisms of *FGB* can affect plasma Fg levels and are also associated with an increased risk of thrombotic disorders, which could be considered as potential biological markers for the development process of IS (Luo et al., 2019). A study using the human serum sample showed that four proteins, including plasminogen, prothrombin, histidine-rich glycoprotein, and Fga, were upregulated in patients with stroke and could be considered as candidate markers to make the diagnosis of IS more accurately and quickly (Lee et al., 2020). In the present study, increased expression of Fg in MCAO rats could lead to the increase of insoluble fibrin and induce the IS. After treatment with TT15, the expression levels of Fga, Fgb, and Fgg all decreased, suggesting that TT15 has an intervention effect on IS.

From the results of MCODE analysis, proteins in cluster I were mainly involved in the complement and coagulation cascade that was regarded as the main pathway for gross saponin of TT to exert an anti-IS effect in our previous study (Wang et al., 2021). Cluster II contains four keratins that few studies reported their relation with stroke. But in MS-based proteomic analysis, keratin is often considered a contaminant because keratin from the researchers' skin and hair can be found on all surfaces and dust during sample processing. And many procedures have been recommended in protocols to minimize keratin contamination (Fox et al., 2008; Mellinger et al., 2021). Therefore, the keratins highlighted in this study need to be further confirmed in our future studies.

4.3. Potential treatment pathway for TT15 against MCAO

Joint pathway analysis showed that the most significantly enriched pathway was the response to elevated platelet cytosolic Ca^{2+} and platelet activation with 14 and 15 molecules involved, respectively. The results suggested that the TT15 may exert the anti-IS effect via regulating platelet function.

Hemostasis depends on the adhesion, activation, and aggregation of platelets on the exposed subendothelial extracellular matrix, but this process can also result in the obstruction of diseased vessels. Therefore, precise regulation of platelet activation is necessary to guarantee that it occurs only when necessary. Platelet activation and aggregation are considered key steps in arterial thrombosis and exacerbation. Inhibition of platelet activation appears to be an attractive strategy for stroke prevention (Marquardt et al., 2002). Different agonists can activate platelets via various signaling pathways, which in turn causes an increase in the intracellular Ca^{2+} concentration. Ca^{2+} is an essential second messenger in nearly all cells, which controls a variety of essential cellular functions. (Berridge et al., 2003). Elevated Ca^{2+} concentration in platelets has the potential to influence a number of cellular activation processes, including degranulation and inside-out activation of integrin αIIbβ3, which is necessary for platelet aggregation (Shattil and Brass, 1987). Several *in vivo* studies have indicated that the various Ca^{2+} entry mechanisms are important for pathological thrombus development while having little impact on hemostasis (Varga-Szabo et al., 2009), which makes molecules that regulate Ca^{2+} entrance in platelets an attractive therapeutic target for ischemic cardio- and cerebrovascular events prevention and therapy.

TT15 may alleviate the development procession of IS and protect the cerebral ischemia injury by comprehensively regulating proteins associated with the Ca^{2+} entry and further influencing the platelet activities. Further studies will be needed to validate the findings in this study and make the underlying mechanisms more clearly.

5. Conclusion

In this study, the chemical composition of TT15 was annotated by LC-MS analysis, and 20 compounds were identified. Then the LC-MS-based multi-omics approach was applied to investigate the therapeutic effects of TT15 against IS. A total of 44 metabolites and 51 differential proteins that were greatly regulated by TT15 were screened out. The

joint pathway analysis showed that these differentially regulated molecules were significantly associated with platelet activities, indicating the possible pathway for TT15 against IS. Further investigation should be performed to verify the pathways and related proteins in the neuroprotective actions of TT15 on IS.

CRediT authorship contribution statement

Dandan Xu: Visualization, Investigation, Conceptualization, Methodology, Software, Writing – original draft. **Yang Wang:** Supervision, Conceptualization, Methodology, Software, Writing - review & editing. **Wenjun Guo:** Visualization, Investigation. **Xingxing Li:** Investigation, Data curation. **Yue Liu:** Visualization, Investigation. **Yuqing Han:** Investigation, Data curation. **Qiyan Wei:** Visualization, Investigation. **Yongsheng Wang:** Supervision, Funding acquisition. **Yajuan Xu:** Supervision, Funding acquisition, Project administration.

Declaration of Competing Interest

The authors declare that they have no known competing financial interests or personal relationships that could have appeared to influence the work reported in this paper.

Acknowledgments

The present study was supported by grants from the National Natural Science Foundation of China (Grant No. 81573590 and 82104366), the Natural Science Fund Project of Jilin Province, China (Grant No. 20200201502JC and 2020020073JC), and the Health Technology Innovation Program of Health Commission of Jilin Province, China (Grant No. 2020J100).

Appendix A. Supplementary material

Supplementary data to this article can be found online at https://doi.org/10.1016/j.arabjc.2022.104297.

References

Abildayeva, K., Berbee, J.F., Blokland, A., et al, 2008. Human apolipoprotein C-I expression in mice impairs learning and memory functions. J. Lipid Res. 49, 856–869. https://doi.org/10.1194/jlr.M700518-JLR200.

Abu-Farha, M., Al-Sabah, S., Hammad, M.M., et al, 2020. Prognostic Genetic Markers for Thrombosis in COVID-19 Patients: A Focused Analysis on D-Dimer, Homocysteine and Thromboembolism. Front. Pharmacol. 11,. https://doi.org/10.3389/fphar.2020.587451 587451.

Adibhatla, R.M., Hatcher, J.F., 2007. Role of Lipids in Brain Injury and Diseases. Future Lipidol. 2, 403–422. https://doi.org/10.2217/17460875.2.4.403.

Alawieh, A., Langley, E.F., Tomlinson, S., 2018. Targeted complement inhibition salvages stressed neurons and inhibits neuroinflammation after stroke in mice. Sci. Transl. Med. 10. https://doi.org/10.1126/scitranslmed.aao6459.

Au, A., 2018. Metabolomics and Lipidomics of Ischemic Stroke. Adv. Clin. Chem. 85, 31–69. https://doi.org/10.1016/bs.acc.2018.02.002.

Barahimi, P., Karimian, M., Nejati, M., et al, 2021. Oxytocin improves ischemic stroke by reducing expression of excitatory amino acid transporter 3 in rat MCAO model. J. Immunoassay Immunochem. 42, 513–524. https://doi.org/10.1080/15321819.2021.1906270.

Berbee, J.F., Vanmierlo, T., Abildayeva, K., et al, 2011. Apolipoprotein CI knock-out mice display impaired memory functions. J. Alzheimers Dis. 23, 737–747. https://doi.org/10.3233/JAD-2010-100576.

Berkowitz, S., Chapman, J., Dori, A., et al, 2021. Complement and Coagulation System Crosstalk in Synaptic and Neural Conduction in the Central and Peripheral Nervous Systems. Biomedicines. 9,. https://doi.org/10.3390/biomedicines9121950 1950.

Berridge, M.J., Bootman, M.D., Roderick, H.L., 2003. Calcium signalling: dynamics, homeostasis and remodelling. Nat. Rev. Mol. Cell Biol. 4, 517–529. https://doi.org/10.1038/nrm1155.

Caplan, L.R., Biousse, V., 2004. Cervicocranial Arterial Dissections. J. Neuroophthalmol. 24, 299–305. https://doi.org/10.1097/00041327-200412000-00007.

Chen, Y., Guillemin, G.J., 2009. Kynurenine Pathway Metabolites in Humans: Disease and Healthy States. Int. J. Tryptophan Res. 2, 1–19. https://doi.org/10.4137/ijtr.s2097.

Chen, H., Qi, S., Shen, J., 2017. One-Compound-Multi-Target: Combination Prospect of Natural Compounds with Thrombolytic Therapy in Acute Ischemic Stroke. Curr. Neuropharmacol. 15, 134–156. https://doi.org/10.2174/1570159x14666160620102.

Chen, H., He, Y., Chen, S., et al, 2020. Therapeutic targets of oxidative/nitrosative stress and neuroinflammation in ischemic stroke: Applications for natural product efficacy with omics and systemic biology. Pharmacol. Res. 158, 104877. https://doi.org/10.1016/j.phrs.2020.104877.

Cherian, L., Chacko, G., Goodman, C., et al, 2003. Neuroprotective effects of L-arginine administration after cortical impact injury in rats: dose response and time window. J. Pharmacol. Exp. Ther. 304, 617–623. https://doi.org/10.1124/jpet.102.043430.

Cherian, L., Robertson, C.S., 2003. L-Arginine and Free Radical Scavengers Increase Cerebral Blood Flow and Brain Tissue Nitric Oxide Concentrations after Controlled Cortical Impact Injury in Rats. J. Neurotrauma. 20, 77–85. https://doi.org/10.1089/08977150360517209.

Chong, J., Soufan, O., Li, C., et al, 2018. MetaboAnalyst 4.0: towards more transparent and integrative metabolomics analysis. Nucleic Acids Res. 46, W486–W494. https://doi.org/10.1093/nar/gky310.

Dalakas, M.C., Alexopoulos, H., Spaeth, P.J., 2020. Complement in neurological disorders and emerging complement-targeted therapeutics. Nat. Rev. Neurol. 16, 601–617. https://doi.org/10.1038/s41582-020-0400-0.

Fluri, F., Schuhmann, M.K., Kleinschnitz, C., 2015. Animal models of ischemic stroke and their application in clinical research. Drug Des. Devel. Ther. 9, 3445–3454. https://doi.org/10.2147/DDDT.S56071.

Fox, K., Castanha, E., Fox, A., et al, 2008. Human K10 epithelial keratin is the most abundant protein in airborne dust of both occupied and unoccupied school rooms. J. Environ. Monit. 10, 55–59. https://doi.org/10.1039/b714802j.

Fuior, E.V., Gafencu, A.V., 2019. Apolipoprotein C1: Its Pleiotropic Effects in Lipid Metabolism and Beyond. Int. J. Mol. Sci. 20,. https://doi.org/10.3390/ijms20235939 5939.

Gomez-Arboledas, A., Acharya, M.M., Tenner, A.J., 2021. The Role of Complement in Synaptic Pruning and Neurodegeneration. Immunotargets Ther. 10, 373–386. https://doi.org/10.2147/ITT.S305420.

Guo, W., Wang, Y., Fan, M., et al, 2020. Integrating metabolomics and network pharmacology to explore the protective effect of gross saponins of Tribulus terrestris L. fruit against ischemic stroke in rat. J. Ethnopharmacol. 263,. https://doi.org/10.1016/j.jep.2020.113202 113202.

Kamburov, A., Cavill, R., Ebbels, T.M., et al, 2011. Integrated pathway-level analysis of transcriptomics and metabolomics data with IMPaLA. Bioinformatics 27, 2917–2918. https://doi.org/10.1093/bioinformatics/btr499.

Kopyta, I., Sarecka-Hujar, B., Sordyl, J., et al, 2014. The role of genetic risk factors in arterial ischemic stroke in pediatric and adult

patients: a critical review. Mol. Biol. Rep. 41, 4241–4251. https://doi.org/10.1007/s11033-014-3295-2.

Koster, T., Rosendaal, F.R., Reitsma, P.H., et al, 1994. Factor VII and Fibrinogen Levels äs Risk Factors for Venous Thrombosis. Thromb. Haemost. 71, 719–722. https://doi.org/10.1055/s-0038-1642511.

Krishnamoorthy, A., Ajay, A.K., Hoffmann, D., et al, 2011. Fibrinogen beta-derived Bbeta(15–42) peptide protects against kidney ischemia/reperfusion injury. Blood 118, 1934–1942. https://doi.org/10.1182/blood-2011-02-338061.

Lee, J., Mun, S., Park, A., et al, 2020. Proteomics Reveals Plasma Biomarkers for Ischemic Stroke Related to the Coagulation Cascade. J. Mol. Neurosci. 70, 1321–1331. https://doi.org/10.1007/s12031-020-01545-4.

Ludhiadch, A., Vasudeva, K., Munshi, A., 2020. Establishing molecular signatures of stroke focusing on omic approaches: a narrative review. Int. J. Neurosci. 130, 1250–1266. https://doi.org/10.1080/00207454.2020.1732964.

Luo, H., Li, X., Jiang, A., et al, 2019. Associations of beta-Fibrinogen Polymorphisms with the Risk of Ischemic Stroke: A Meta-analysis. J. Stroke Cerebrovas. Dis. : Off. J. Nat. Stroke Assoc. 28, 243–250. https://doi.org/10.1016/j.jstrokecerebrovasdis.2018.09.007.

Ma, Y., Liu, Y., Zhang, Z., et al, 2019. Significance of Complement System in Ischemic Stroke: A Comprehensive Review. Aging Dis. 10, 429–462. https://doi.org/10.14336/AD.2019.0119.

Marquardt, L., Ruf, A., Mansmann, U., et al, 2002. Course of platelet activation markers after ischemic stroke. Stroke 33, 2570–2574. https://doi.org/10.1161/01.str.0000034398.34938.20.

Mattson, M.P., 2008. Glutamate and neurotrophic factors in neuronal plasticity and disease. Ann. N. Y. Acad. Sci. 1144, 97–112. https://doi.org/10.1196/annals.1418.005.

Mellinger, A.L., McCoy, K., Minior, D.A.T., et al, 2021. Discovery proteomics of human placental tissue. Rapid Commun. Mass Spectrom. e9189. https://doi.org/10.1002/rcm.9189.

Muralikrishna Adibhatla, R., Hatcher, J.F., 2006. Phospholipase A2, reactive oxygen species, and lipid peroxidation in cerebral ischemia. Free Radic. Biol. Med. 40, 376–387. https://doi.org/10.1016/j.freeradbiomed.2005.08.044.

Neuhaus, A.A., Couch, Y., Hadley, G., et al, 2017. Neuroprotection in stroke: the importance of collaboration and reproducibility. Brain. 140, 2079–2092. https://doi.org/10.1093/brain/awx126.

Ormstad, H., Verkerk, R., Aass, H.C., et al, 2013. Inflammation-induced catabolism of tryptophan and tyrosine in acute ischemic stroke. J. Mol. Neurosci. 51, 893–902. https://doi.org/10.1007/s12031-013-0097-2.

Reynaert, N.L., Ckless, K., Guala, A.S., et al, 2006. In situ detection of S-glutathionylated proteins following glutaredoxin-1 catalyzed cysteine derivatization. Biochim. Biophys. Acta. 1760, 380–387. https://doi.org/10.1016/j.bbagen.2006.01.006.

Ricklin, D., Hajishengallis, G., Yang, K., et al, 2010. Complement: a key system for immune surveillance and homeostasis. Nat. Immunol. 11, 785–797. https://doi.org/10.1038/ni.1923.

Shattil, S.J., Brass, L.F., 1987. Induction of the fibrinogen receptor on human platelets by intracellular mediators. J. Biol. Chem. 262, 992–1000. https://doi.org/10.1016/s0021-9258(19)75739-1.

Shin, T.H., Lee, D.Y., Basith, S., et al, 2020. Metabolome Changes in Cerebral Ischemia. Cells. 9, 1630. https://doi.org/10.3390/cells9071630.

Thomas, R.J., 1995. Excitatory Amino Acids in Health and Disease. J. Am. Geriatr. Soc. 43, 1279–1289. https://doi.org/10.1111/j.1532-5415.1995.tb07407.x.

Van Guldener, C., Nanayakkara, P.W., Stehouwer, C.D., 2007. Homocysteine and asymmetric dimethylarginine (ADMA): biochemically linked but differently related to vascular disease in chronic kidney disease. Clin. Chem. Lab. Med. 45, 1683–1687. https://doi.org/10.1515/CCLM.2007.340.

Varga-Szabo, D., Braun, A., Nieswandt, B., 2009. Calcium signaling in platelets. J. Thromb. Haemost. 7, 1057–1066. https://doi.org/10.1111/j.1538-7836.2009.03455.x.

Veerhuis, R., Nielsen, H.M., Tenner, A.J., 2011. Complement in the brain. Mol. Immunol. 48, 1592–1603. https://doi.org/10.1016/j.molimm.2011.04.003.

Victor Nadler, J., Wang, A., Hakim, A., 1988. Toxicity of L-proline toward rat hippocampal neurons. Brain Res. 456, 168–172. https://doi.org/10.1016/0006-8993(88)90358-7.

Wang, Y., Guo, W., Liu, Y., et al, 2019. Investigating the Protective Effect of Gross Saponins of Tribulus terrestris Fruit against Ischemic Stroke in Rat Using Metabolomics and Network Pharmacology. Metabolites. 9,. https://doi.org/10.3390/metabo9100240 240.

Wang, Y., Guo, W., Xie, S., et al, 2021. Multi-omics analysis of brain tissue metabolome and proteome reveals the protective effect of gross saponins of Tribulus terrestris L. fruit against ischemic stroke in rat. J. Ethnopharmacol. 278, 114280. https://doi.org/10.1016/j.jep.2021.114280.

Wiesinger, H., 2001. Arginine metabolism and the synthesis of nitric oxide in the nervous system. Prog. Neurobiol. 64, 365–391. https://doi.org/10.1016/s0301-0082(00)00056-3.

Xie, Q., Li, H., Lu, D., et al, 2021a. Neuroprotective Effect for Cerebral Ischemia by Natural Products: A Review. Front. Pharmacol. 12,. https://doi.org/10.3389/fphar.2021.607412 607412.

Xie, W., Wang, X., Xiao, T., et al, 2021b. Protective Effects and Network Analysis of Ginsenoside Rb1 Against Cerebral Ischemia Injury: A Pharmacological Review. Front. Pharmacol. 12,. https://doi.org/10.3389/fphar.2021.604811 604811.

Yang, L., Qian, J., Yang, B., et al, 2021. Challenges and Improvements of Novel Therapies for Ischemic Stroke. Front. Pharmacol. 12,. https://doi.org/10.3389/fphar.2021.721156 721156.

Yang, P., Song, X., Chen, N., 2016. Advances in pharmacological studies of Panax notoginseng saponins on brain ischemia-reperfusion injury. Acta Pharm. Sin. 51, 1039–1046. https://doi.org/10.16438/j.0513-4870.2015-0991.

Zhou, Y., Zhou, B., Pache, L., et al, 2019. Metascape provides a biologist-oriented resource for the analysis of systems-level datasets. Nat. Commun. 10, 1523. https://doi.org/10.1038/s41467-019-09234-6.

Zhu, T., Wang, L., Feng, Y., et al, 2020. Classical Active Ingredients and Extracts of Chinese Herbal Medicines: Pharmacokinetics, Pharmacodynamics, and Molecular Mechanisms for Ischemic Stroke. Oxid. Med. Cell. Longev. 2021, 8868941. https://doi.org/10.1155/2021/8868941.